Thermo-Reversible Formation of Wormlike Micelles with a Microphase-Separated Corona from a Semicrystalline Triblock Terpolymer

Holger Schmalz,*,† Joachim Schmelz,† Markus Drechsler,† Jiayin Yuan,† Andreas Walther,† Kristian Schweimer,‡ and Adriana M. Mihut§

Makromolekulare Chemie II, Biopolymere, and Physikalische Chemie I, Universität Bayreuth, D-95440 Bayreuth, Germany

Received August 16, 2007; Revised Manuscript Received February 6, 2008

ABSTRACT: The thermo-reversible formation of wormlike micelles from a polystyrene-*block*-polyethylene-*block*-poly(methyl methacrylate) (PS-*b*-PE-*b*-PMMA) triblock terpolymer with a crystallizable middle block in organic media is presented. The formation of wormlike micelles is rather unexpected, because PE containing diblock copolymers usually form platelet-like structures. Transmission electron microscopy (TEM) investigations revealed a core−corona structure for the wormlike micelles. The core is formed by crystalline PE domains, and the soluble corona exhibits a patched structure composed of microphase-separated PS and PMMA chains. Microphase separation of the coronal chains was proven by 2D ^{1}H nuclear Overhauser effect spectroscopy (NOESY) and TEM investigations of selectively stained samples. A combination of various techniques, such as differential scanning calorimetry (DSC), dynamic light scattering (DLS), and scanning force microscopy (SFM), indicated that the wormlike micelles might be formed by crystallization-induced aggregation of spherical micelles upon cooling. The presented approach opens an alternative way to produce anisotropic polymer nanostructures with a microphase-separated corona.

Introduction

Self-assembly of amorphous (coil−coil) block copolymers in selective solvents for one of the blocks has been investigated in detail during the past few years.[1] Commonly, spherical micelles were obtained. Other morphologies (cylinders and vesicles) have been observed particularly in so-called "crew-cut" systems, i.e., the dimensions of the core are bigger than those of the corona, with the possibility to tune the structure, e.g., by varying solvent composition, pH, temperature, or salinity.[2] However, these systems usually require dialysis from a common solvent for both blocks against a selective solvent, or a mixture of common and selective solvents has to be used. Cylindrical micelles were reported for block copolymers directly soluble in a selective solvent for one of the blocks, too; i.e., the weight fraction of the soluble block is sufficiently high to promote a direct dissolution without the need of a common solvent.[3] In addition, there are several reports on ABC triblock terpolymers forming cylindrical micelles in block-selective solvents.[4] In comparison to the numerous publications about coil−coil block copolymers, the self-assembly of block copolymers, where the insoluble block is able to self-organize by crystallization, i.e., crystalline−coil diblock copolymers, is less extensively investigated and yet not completely understood.

Theoretical work on crystalline−coil diblock copolymers predicts the stability of spherical, cylindrical, and lamellar structures.[5] It is noted that the core of the spherical micelles is anisotropic (comparable to a cylindrical shape) because of the chain folding of the crystallizable block. Thus, a more precise nomenclature might be "hockey-puck" micelles, which is used for the description of rod−coil diblock copolymer micelles.[6,7] The same situation applies for cylindrical micelles, where the crystalline core adopts a shape comparable to a rectangular prism. Gast et al. used a self-consistent mean field (SCF) approach in combination with a chain-folding model to calculate the equilibrium structures of crystalline−coil platelets in solution.[8] They found a good agreement between theory and experimental results for polystyrene-*block*-poly(ethylene oxide) (PS-*b*-PEO) and polyethylene-*block*-poly(ethylene-*alt*-propylene) (PE-*b*-PEP) platelets suspended in cyclopentane and *n*-decane, respectively. The morphology of the formed aggregates is controlled by three main factors: the enthalpy of fusion of the crystallizable block, the interfacial energy between the crystalline core and the solvent, and the conformational entropy of the amorphous block (free-energy penalty because of chain stretching). The interplay of these factors, i.e., minimization of the total free energy, determines the final structure, and there is a strong influence of chain folding of the crystalline block. For the semicrystalline core of a spherical micelle, there are two types of interfaces: the fold interface and the lateral interface. The enthalpy of fusion generally increases with a decreasing chain folding. However, this results in an increased lateral surface area; i.e., aggregation of spherical micelles into platelets is favored to minimize the lateral interfacial energy. On the other hand, the soluble amorphous block is densely grafted on the fold interface. Consequently, the amorphous chains have to be more stretched with a decreasing chain folding, i.e., increasing grafting density. This results in a loss of conformational entropy, exerting a positive contribution to the total free energy.

Self-assembly of crystalline−coil diblock copolymers generally results in the formation of thin platelet-like structures, with flat chain-folded crystalline domains sandwiched between brush layers of the soluble block. One of the most intensively studied system is based on PE and PEP. Several copolymers with varying molecular weight, PE content, and architecture were investigated and shown to form platelet-like structures.[8−10] PS-*b*-PEO diblock copolymers usually form large platelet-like structures in organic media.[11] However, the formed structures were found to be very sensitive to traces of water; i.e., the formation of spherical micelles is favored with an increasing water content.[12]

* To whom correspondence should be addressed. E-mail: holger.schmalz@uni-bayreuth.de.
† Makromolekulare Chemie II.
‡ Biopolymere.
§ Physikalische Chemie I.

10.1021/ma702417y CCC: $40.75
Published on Web 04/05/2008

Spherical and cylindrical structures are rarely observed and basically only for specific systems. It is noted that cylindrical structures were observed for rod−coil block copolymers, which can be attributed to the packing of the rigid insoluble block in the core.[13] However, these systems are fundamentally different from crystalline−coil systems because chain folding does not play a role. PE/PEP diblock copolymer stars form cylindrical micelles when PE is located in the star center. In contrast, if PE is located at the star rim, platelets are formed.[10] Elongated structures were also observed for cocrystallization (stereocomplexation) of enantiomeric diblock copolymers based on poly(ethylene oxide)-*block*-poly(L/D-lactide) and block copolymers composed of poly(ε-caprolactone)/poly(L/D-lactide) (AB and ABA type) in selective solvents.[14,15] Organometallic block copolymers based on poly(ferrocenyldimethylsilane) (PFDMS) are remarkable systems forming rigid cylindrical micelles with a high aspect ratio but, on the other hand, are also very special because of the organometallic polymer used. Various PFDMS-*block*-coil diblock copolymers have been synthesized with the coil blocks consisting of polydimethylsiloxane (PDMS), polyisoprene (PI), PEO, poly(2-vinyl pyridine) (P2VP), poly(methyl methacrylate) (PMMA), and poly(*N*,*N*-dimethylaminoethyl methacrylate) (PDMAEMA).[16–19] In addition, a reversible transition from cylindrical micelles to hollow nanotubes was observed for a PFDMS-*b*-PDMS with a block ratio of 1:12.[20,21] Replacing the semicrystalline PFDMS block by an amorphous organometallic block, e.g., poly(ferrocenylmethylphenylsilane) (PFMPS), revealed that crystallization is the main driving force for the formation of cylindrical micelles, because spherical micelles were formed exclusively for amorphous polyferrocene blocks.[18] This is supported by aggregation studies of PFDMS-*b*-P2VP in alcohols.[19] Spherical micelles with an amorphous PFDMS core were formed in methanol, as revealed by wide-angle X-ray scattering. In contrast, cylindrical micelles with a crystalline PFDMS core were observed in isopropanol. However, recent NMR investigations on PFDMS-*b*-PMMA cylindrical micelles revealed some mobility of the PFDMS chains in the core, suggesting that the core is not in a crystalline state.[17] The interplay of various factors determining the final morphology clearly shows the complexity of these systems.

Concerning the self-assembly of semicrystalline triblock copolymers in solution, only a few examples are available in the literature. Mostly, ABA-type copolymers have been studied, e.g., with PEO as A blocks and poly(α-methyl styrene) or poly(propylene oxide) as B blocks, both forming platelet-like structures.[22] Kimura et al. investigated the self-organization of PEO-*block*-poly(L-lactide)-based di- and triblock copolymers during structural changes from discoid nanoparticles in aqueous dispersion to band structures after deposition and subsequent annealing on a mica substrate.[23] Flower-like superstructures were observed for PFDMS-*b*-PDMS-*b*-PFDMS triblock copolymers in *n*-hexane, a selective solvent for the PDMS block, by Winnik and Manners et al.[24] The same group studied coil−crystalline−coil PFP-*b*-PFDMS-*b*-PDMS ABC triblock terpolymers [PFP = poly(ferrocenylphenylphosphine)] with short PFP blocks of variable length.[25] Dependent upon the PFP block length, either cylindrical micelles with a crystalline PFDMS core (short PFP block) or spherical micelles (long PFP block) with an amorphous core were formed.

The motivation of this work was the question whether the use of ABC triblock terpolymers with a crystallizable middle block opens up a more general route to produce spherical or cylindrical (wormlike) aggregates driven by crystallization. The attachment of two chemically different polymers to the crystalline block enlarges the number of parameters, e.g., composition, that can be adjusted to gain a specific morphology. Particularly, the structure of the corona, i.e., mixed or microphase-separated, might be easily tuned by varying the incompatibility of the A and C blocks. This might open a new route to polymer nanostructures with a microphase-separated corona, e.g., Janus-type (two-faced) or patched.[26] The advantage over existing methods for Janus-type structures, such as the template-assisted approach (Janus micelles, cylinders, and discs)[27,28] or the copolymerization of macromonomers (Janus cylinders),[29] is the comparatively easy preparation by simply cooling a solution of the polymer to induce crystallization.

In this paper, we show that wormlike micelles with a patched corona can be produced from a polystyrene-*block*-polyethylene-*block*-poly(methyl methacrylate) ($S_{39}E_{21}M_{40}^{91.5}$) triblock terpolymer via crystallization-induced self-assembly in organic media. The morphology of the formed aggregates has been investigated using various microscopy techniques, e.g., transmission electron microscopy (TEM), cryogenic transmission electron microscopy (cryo-TEM), and scanning force microscopy (SFM). Two-dimensional nuclear magnetic resonance (NMR) techniques in combination with TEM of selectively stained samples have been applied to prove the phase separation in the corona.

Experimental Section

Polymerization. Polymerization was carried out in a thermostatted laboratory autoclave (Büchi AG) under a dry nitrogen atmosphere. The polystyrene-*block*-poly(1,4-butadiene)-*block*-poly(methyl methacrylate) (PS-*b*-PB-*b*-PMMA) triblock terpolymer was synthesized via sequential anionic polymerization of the corresponding monomers in toluene. The use of a nonpolar solvent is essential to produce a polybutadiene block with a high content of 1,4-addition, which is indispensable to obtain the corresponding "pseudo-polyethylene" structure after hydrogenation. First, styrene was polymerized at 24 °C for 2 h using *sec*-BuLi as the initiator. The reaction mixture was then cooled to 10 °C, and butadiene was added. Butadiene was allowed to polymerize at 40 °C for 3 h followed by cooling to −10 °C. After subsequent addition of a DME/*i*BAl(BHT)$_2$ mixture [DME, 1,2-dimethyoxyethane; *i*BAl(BHT)$_2$, di[2,6-di(*tert*-butyl)-4-methyl phenoxy]isobutyl aluminum] and MMA, the reaction was kept at −10 °C for 1 h. Finally, MMA polymerization was conducted at 25 °C for 4 h followed by termination with degassed methanol. A more detailed polymerization procedure and information about used materials are given elsewhere.[30]

The reaction mixture was extracted with a 2% aqueous H_2SO_4 by rigorous stirring for 1 h (extraction of the catalyst). The organic phase was separated and washed with distilled water to remove residual H_2SO_4. The polymer was isolated by precipitation into isopropanol. Small traces of PS precursor resulting from termination (ca. 3 wt %) were removed by extraction with cyclohexane, a selective solvent for PS and PB, overnight.

The composition and molecular weight of the produced triblock terpolymer $S_{39}B_{21}M_{40}^{91}$ (the subscripts denote the mass fraction in percent, and the superscript gives the number-average molecular weight M_n in kg/mol) were determined via ^{1}H NMR in $CDCl_3$ (Bruker AC 250 spectrometer) using the molecular weight of the PS precursor, determined via matrix-assisted laser desorption ionization−time of flight (MALDI−TOF; Bruker Reflex III), for calibration of the NMR signal intensities.

Hydrogenation. The polystyrene-*block*-polyethylene-*block*-poly(methyl methacrylate) ($S_{39}E_{21}M_{40}^{91.5}$) triblock terpolymer was obtained by hydrogenation of the corresponding $S_{39}B_{21}M_{40}^{91}$ precursor. Homogeneous catalytic hydrogenation was carried out in degassed toluene (p.a., Merck, 2 wt % solution of the polymer) at 60 °C and 60 bar H_2 pressure for 3 days using Wilkinson catalyst $(Ph_3P)_3Rh^{I}Cl$ (Aldrich, 1 mol % with respect to the number of double bonds of the PB block). Under the employed conditions, the PB block gets completely hydrogenated as revealed by ^{1}H NMR spectroscopy (Bruker AC 250 spectrometer, results not shown). The polymer was recovered by precipitation into isopropanol. Further

purification was performed to remove residual Wilkinson catalyst by refluxing a solution of the triblock terpolymer in toluene with a small amount of concentrated hydrochloric acid. Precipitation into isopropanol yielded a white powder.

Preparation of Solutions. Stock solutions of the $S_{39}E_{21}M_{40}^{91.5}$ triblock terpolymer in toluene (1 g/L, and 10 g/L) with a defined thermal history were prepared by dissolving the polymer at elevated temperatures (ca. 60 °C). Because of the crystallinity of the polyethylene (PE) block, the solubility at room temperature is only moderate and takes at least 1 day. Furthermore, dissolving the polymer at high temperatures ensures that any thermal history is eliminated, because differential scanning calorimetry (DSC) measurements on a 10 g/L toluene solution indicated a melting point of the PE block at about 50 °C. To achieve a well-defined structure formation process upon cooling, the toluene solutions were cooled from 60 to 20 °C under gentle stirring at a rate of 0.5 K/min using a home-build double-jacketed flask connected to a LAUDA Ecoline RE306 thermostat. During cooling of the isotropic solution, the appearance of a bluish color was observed at ca. 20 °C. This can be ascribed to the light scattering of large objects formed, having sizes in the wavelength range of visible light (Tyndall effect). The bluish color disappeared upon heating to ca. 50 °C; i.e., break-up of large aggregates occurred and reversibly reappeared when the sample was cooled again to 20 °C.

Solutions in tetrahydrofuran (THF) (10 g/L) were prepared by dissolving the polymer at ca. 60 °C. After the polymer was completely dissolved, the solution was kept at 60 °C for 1 h and subsequently quenched to room temperature by immersing into a water bath.

Solutions of $S_{39}E_{21}M_{40}^{91.5}$ in acetone (1 g/L), a selective solvent for PMMA, were prepared by dialysis of the 1 g/L stock solution in toluene against acetone for 3 days. To keep a constant concentration, a QuixSep Microdialyzer (volume 5 mL, Carl Roth) covered with a Spectra/Por 1 dialysis membrane (MWCO 6−8 kg/mol, Spectrum Laboratories) was used. The dialysate was replaced 2 times by fresh acetone to ensure a complete exchange of solvents.

All experiments were performed using the stock solutions in toluene or THF with a defined thermal history, as described above. The solutions were allowed to equilibrate for at least 2 days at room temperature before use. If lower concentrations were required, the stock solutions were diluted accordingly.

Two-Dimensional ^{1}H NMR Nuclear Overhauser Effect Spectroscopy (NOESY). ^{1}H NMR spectra of the micellar solutions in toluene-d_8 (10 g/L) were recorded at 300 K on a Bruker Avance 800 MHz spectrometer equipped with a cryogenically cooled probe. The 2D ^{1}H NOESY spectrum (mixing time of 250 ms) was recorded with 80 scans and 2048 × 128 complex data points. The spectral width was 7200 Hz, and the recycle delay was 2.5 s. Sample preparation was conducted according to the procedure given in the Preparation of Solutions section to compare samples with an identical thermal history.

Differential Scanning Calorimetry (DSC). For thermal analysis of the $S_{39}E_{21}M_{40}^{91.5}$ triblock terpolymer in the bulk state, a Perkin-Elmer Pyris 1 with a CCA 7 liquid nitrogen cooling device was used. A two-point calibration with decane and indium was applied, and the measurement was performed at a scanning rate of 10 K/min. The displayed heating trace corresponds to the second heating run to exclude effects resulting from any previous thermal history of the sample. The degree of crystallinity for the PE block was calculated using the heat of fusion for a 100% crystalline PE of $\Delta H^0_m = 276.98$ J/g.[31] Measurements on toluene solutions of $S_{39}E_{21}M_{40}^{91.5}$ (10 g/L) were performed using a Setaram Micro-DSC III at a scanning rate of 0.5 K/min. The Micro-DSC allows for measurements with an extremely high sensitivity using sample masses up to 1 g and, hence, the detection of phase transitions with very small enthalpy values.

Scanning Force Microscopy (SFM). SFM images were taken on a Digital Instruments Dimension 3100 microscope operated in TappingMode. Samples were prepared on polished silicon wafers by dip coating from a 0.05 g/L solution of the $S_{39}E_{21}M_{40}^{91.5}$ triblock terpolymer in toluene, prepared by dilution of the corresponding stock solution (1 g/L) with a defined thermal history. For sample preparation at 60 °C, dip coating and subsequent drying was conducted in a drying oven (Heraeus) operated at 60 ± 1 °C. The given values for the average diameter (value not deconvoluted for tip size) and height were determined by cross-sectional analysis of at least 30 different wormlike micelles (NanoScope 5.13r10sr1 software).

Dynamic Light Scattering (DLS). DLS was performed on an ALV DLS/SLS-SP 5022F compact goniometer system with an ALV 5000/E cross-correlator and a He−Ne laser ($\lambda_0 = 632.8$ nm). All measurements were performed on a 1 g/L solution of $S_{39}E_{21}M_{40}^{91.5}$ in toluene. Because of the large size of the aggregates formed at room temperature, the solutions were not filtered prior to measurement to avoid any loss of material. For temperature-dependent measurements, the toluene bath of the instrument was thermostatted using a LAUDA Proline RP 845 thermostat. Prior to measurement, the system was allowed to equilibrate for at least 10 min after reaching the targeted temperature. Presented scattering intensity data correspond to an average of five measurements.

Transmission Electron Microscopy (TEM). Samples were prepared by placing a drop of a dilute solution of $S_{39}E_{21}M_{40}^{91.5}$ (0.5–1 g/L in toluene or acetone) on a carbon-coated copper grid. After 30 s, excess solution was removed by blotting with a filter paper. Subsequently, elastic bright-field TEM was performed on a Zeiss 922OMEGA EFTEM (Zeiss NTS GmbH, Oberkochen, Germany) operated at 200 kV. Staining was performed with RuO_4 vapor for 60 min. RuO_4 is known to selectively stain PS; i.e., PS domains are expected to appear darker compared to PMMA domains, which would enable to distinguish between PS and PMMA domains in the micelle corona. The average diameter of the observed wormlike micelles was determined by cross-sectional darkness analysis of at least 30 micelles using the line profile tool in the Gatan Digital Micrograph 3.15 for GMS 1.5 software (integration depth of 100 pixels).

Cryogenic Transmission Electron Microscopy (Cryo-TEM). For cryo-TEM studies, a 2 μL droplet of the 1 g/L solution of $S_{39}E_{21}M_{40}^{91.5}$ in THF was put on a lacey carbon-coated copper grid, where most of the liquid was removed with blotting paper, leaving a thin film stretched over the lace. The specimens were instantly vitrified by rapid immersion into liquid nitrogen and cooled to approximately 77 K using a temperature-controlled freezing unit (Zeiss Cryobox, Zeiss NTS GmbH, Oberkochen, Germany). The temperature was monitored and kept constant in the chamber during all of the sample preparation steps. After freezing, the specimen was inserted into a cryo-transfer holder (CT3500, Gatan, München, Germany) and transferred to a Zeiss 922OMEGA EFTEM (Zeiss NTS GmbH, Oberkochen, Germany). Examinations were carried out at temperatures around 95 K. The TEM was operated at an acceleration voltage of 200 kV. Zero-loss filtered micrographs ($\Delta E = 0$ eV) were recorded under reduced dose conditions (100–1000 e/nm^2). All images were registered digitally by a bottom-mounted CCD camera system (Ultrascan 1000, Gatan) combined and processed with a digital image processing system (Gatan Digital Micrograph 3.15 for GMS 1.5).

Wide-Angle X-ray Diffraction (WAXD). The WAXD measurement was carried out at the ID2 beam line at the European Synchrotron Radiation Facility (ESRF, Grenoble, France). The wavelength of the used X-rays was $\lambda = 0.1$ nm. Measurements were performed on a 50 g/L solution of the triblock terpolymer in toluene at 20 °C. The sample was prepared in a manner similar to the procedure given in the Preparation of Solutions section.

Results and Discussion

Synthesis and Characterization of the $S_{39}E_{21}M_{40}^{91.5}$ Triblock Terpolymer. The polystyrene-*block*-polyethylene-*block*-poly(methyl methacrylate) ($S_{39}E_{21}M_{40}^{91.5}$) triblock terpolymer was synthesized by catalytic hydrogenation of a corresponding polystyrene-*block*-poly(1,4-butadiene)-*block*-poly(methyl methacrylate) ($S_{39}B_{21}M_{40}^{91}$) precursor using Wilkinson catalyst [$(Ph_3P)_3Rh^ICl$]. In the used nomenclature, the subscript numbers

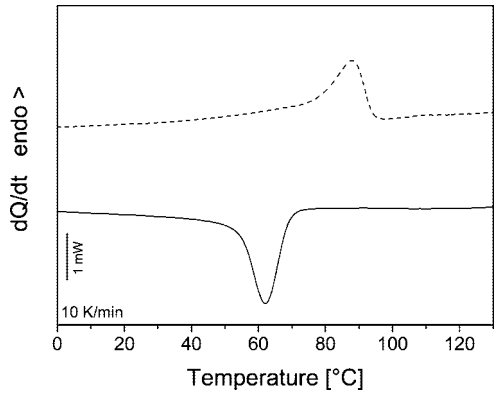

Figure 1. DSC heating (- - -) and cooling (—) traces of a $S_{39}E_{21}M_{40}^{91.5}$ bulk sample monitored at a scanning rate of 10 K/min.

denote the mass fraction in percent and the superscript number gives the number-average molecular weight of the triblock terpolymer in kg/mol. The $S_{39}B_{21}M_{40}^{91}$ triblock terpolymer ($M_w/M_n = 1.04$) was prepared via sequential anionic polymerization in toluene with *sec*-BuLi as the initiator.[30] Polymerization was performed in a nonpolar solvent to obtain a high content of 1,4-addition for the polybutadiene block, which is indispensable to obtain the corresponding "pseudo-polyethylene" structure after hydrogenation. A more detailed description of the synthetic procedure can be found in the Experimental Section.

Figure 1 shows a DSC measurement on a $S_{39}E_{21}M_{40}^{91.5}$ bulk sample. The semicrystalline polyethylene (PE) middle block shows a melting transition at $T_{m,\ peak} = 88.0$ °C and a corresponding crystallization temperature upon cooling at $T_{c,\ peak} = 62.0$ °C. The degree of crystallinity (α) is 24.9%. These values are typical for PE-containing block copolymers obtained via hydrogenation of 1,4-polybutadiene.[32] Because of the synthetic procedure, the polybutadiene block contains 10 mol % 1,2 units. Thus, upon hydrogenation, a PE block with 5.2 mol % ethyl branches (1-butene units) is obtained, corresponding to 2.6 ethyl branches per 100 C atoms. The glass transition temperatures of the PS and PMMA blocks were determined by DSC measurements on the $S_{39}B_{21}M_{40}^{91}$ precursor to 107 and 135 °C, respectively.[30]

Morphology of Aggregates in Solution. For self-assembly studies in organic media, stock solutions in toluene (1 and 10 g/L) and THF (10 g/L) were prepared by dissolving the polymer at elevated temperatures (ca. 60 °C) followed by controlled cooling from 60 to 20 °C at 0.5 K/min for the toluene solutions and quenching from 60 to 20 °C for the THF solution, respectively (for details, see the Experimental Section). The PE block melts at ca. 50 °C in toluene solution; thus, dissolving the polymer at about 60 °C eliminates any thermal history that might influence the structure formation upon cooling. The solutions were allowed to equilibrate at 20 °C for at least 2 days prior to TEM or SFM investigations. DLS experiments revealed that structure formation is completed within 1 day; i.e., no significant change in the intensity of scattered light is observed after 1 day (Figure S1 in the Supporting Information). Figure 2A shows a cryo-TEM micrograph of the objects formed upon quenching a THF solution of $S_{39}E_{21}M_{40}^{91.5}$ from 60 to 20 °C. Thin elongated structures, appearing darker in the TEM micrograph, can be clearly detected. The structure formation upon cooling is controlled by the PE block that crystallizes and becomes insoluble. Thus, the observed objects can be attributed to wormlike micelles with a semicrystalline PE core and a soluble corona formed by PS and PMMA chains. Because of the low scattering contrast of the corona with respect to the pure solvent, the corona structure cannot be resolved in cryo-TEM.

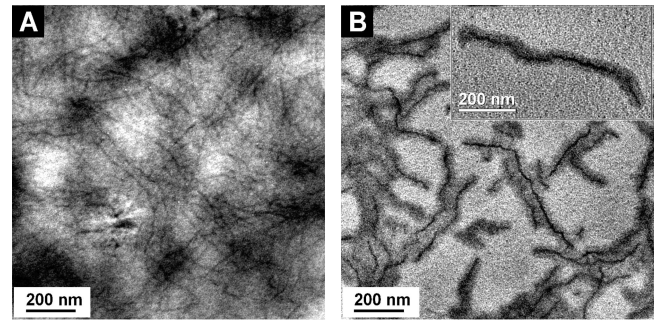

Figure 2. Cryo-TEM micrograph of a 1 g/L solution of $S_{39}E_{21}M_{40}^{91.5}$ in THF (A) and TEM micrograph of $S_{39}E_{21}M_{40}^{91.5}$ wormlike micelles deposited on a carbon-coated copper grid by drop coating of a 1 g/L toluene solution (B).

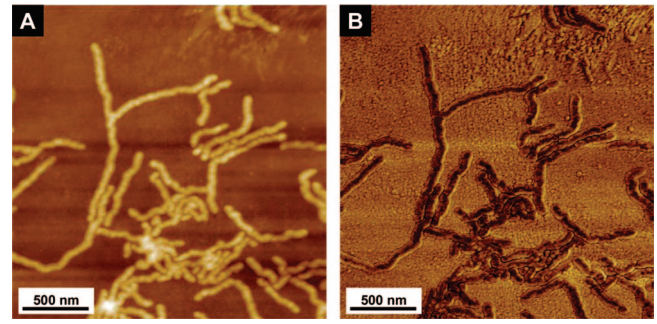

Figure 3. SFM topography and phase-contrast images of $S_{39}E_{21}M_{40}^{91.5}$ wormlike micelles (A, z range = 35 nm; B, $\Delta\varphi = 30°$); the sample was prepared by dip coating from a 0.05 g/L solution in toluene onto a silicon wafer.

The morphology is more evident from Figure 2B, showing a TEM micrograph of the sample prepared by drop coating of a 1 g/L toluene solution onto a carbon-coated copper grid. A core−corona structure is clearly visible, with the semicrystalline PE core showing a higher scattering contrast (appears darker) compared to that of the PS/PMMA corona. The higher contrast of the PE core is related to a more dense packing of chains in a crystallite compared to the amorphous state. A more detailed discussion on the core structure will be given later. The average diameter of the wormlike micelles is 64 ± 2 nm, while the length is rather nonuniform. Consequently, $S_{39}E_{21}M_{40}^{91.5}$ forms wormlike micelles with a semicrystalline PE core and a corona formed by the soluble PS and PMMA chains, regardless of the solvent (THF or toluene) and the cooling rate (quenching or 0.5 K/min).

SFM characterization provided a more detailed insight into the morphology of the formed aggregates. Samples were prepared by dip coating from a 0.05 g/L toluene solution, obtained by dilution of the corresponding stock solution (1 g/L). The topography (Figure 3A) and phase-contrast (Figure 3B) images clearly confirm the wormlike structure.

The diameter of the wormlike micelles ($d = 77 \pm 5$ nm) is rather uniform, which is consistent with TEM results. The higher values obtained by SFM can be attributed to convolution with the SFM tip size[33] and to the known preferential adsorption of PMMA onto polar substrates,[34] i.e., the SiO_x surface of the silicon wafer. The length distribution is relatively broad, ranging from ca. 100 nm to micelles with >1 μm in length. The values are comparable to that found in TEM; i.e., the wormlike micelles are stable against dilution, because solutions for SFM were 20 times higher diluted. This is reasonable, because the micelles can be considered "frozen" below the melting point of the PE block. The height of the wormlike micelles (7.5 ± 0.6 nm) is considerably smaller than the diameter (77 ± 5 nm). A low

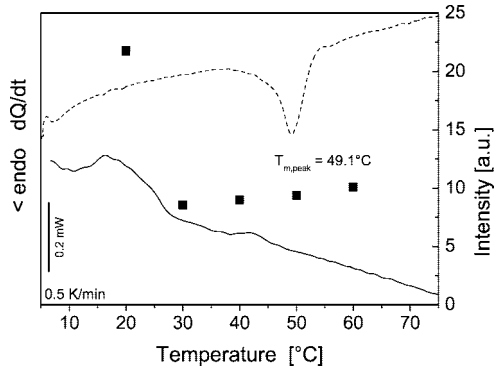

Figure 4. DSC heating (- - -) and cooling (—) traces of a $S_{39}E_{21}M_{40}^{91.5}$ solution in toluene (10 g/L). The squares give the temperature-dependent scattering intensity of a 1 g/L solution of $S_{39}E_{21}M_{40}^{91.5}$ in toluene measured via DLS at a scattering angle $\theta = 95°$ upon cooling from 60 °C.

height/width ratio is commonly observed for cylindrical (wormlike) structures and can be explained by the collapse of the coronal chains on the substrate surface.[35] This effect is even more pronounced when the polymer chains preferentially adsorb on the surface of the used substrate, such as, in our case, the PMMA chains on the SiO_x surface of the silica wafer. Similar results were reported for Janus cylinders (PS/PMMA corona) prepared by a template-assisted approach, starting from SBM triblock terpolymers with a lc (lamellae−cylinder) bulk morphology followed by cross-linking of the PB domains.[28] A closer look to the phase-contrast image (Figure 3B) reveals that the contour of the wormlike micelles is not smooth but shows an undulated structure. A similar observation was recently reported for the cocrystallization of enantiomeric diblock copolymers.[14] It is proposed that the wormlike micelles might be formed by crystallization-induced aggregation of spherical micelles upon cooling. A similar mechanism was suggested for the formation of platelet-like structures,[36] and a comparable sphere−rod transition upon cooling was described for polyferrocenylsilane-based diblock copolymers in selective solvents.[17,18,37]

Mechanism of Self-Assembly. To support the assumption that the wormlike micelles might be formed via crystallization-induced aggregation of spherical micelles, we investigated the structure formation process upon cooling in more detail. DSC measurements on toluene solutions (Figure 4) revealed a melting point of the PE block at $T_{m,\ peak} = 49.1$ °C and a broad crystallization transition between 25 and 10 °C. Melting and crystallization of PE occurred at significantly lower temperatures compared to that of the bulk sample (Figure 1), which can be attributed to a plasticizing effect of toluene. Temperature-dependent DLS showed an increase in scattering intensity at 20 °C upon cooling from 60 °C (Figure 4). Since the refractive index increment (dn/dc) of the terpolymer is not expected to change significantly upon crystallization, this clearly indicates the formation of objects with higher molecular mass via aggregation. Thus, the onset of aggregate formation correlates well with the observed crystallization transition in DSC. The formation of large objects upon cooling could even be observed by visual inspection of more concentrated toluene solutions (10 g/L). Initially transparent solutions at 60 °C became bluish at around 20 °C (Tyndall effect). The Tyndall effect disappeared again after heating to about 50 °C, the melting point of PE according to DSC. Consequently, the formation of wormlike micelles is closely connected to the crystallization of the PE block and revealed to be fully reversible.

Further details on the aggregation mechanism were obtained from SFM investigations on samples prepared by dip coating from a 0.05 g/L toluene solution at 60 °C and after subsequent cooling at 20 °C. Figure 5A clearly indicates the presence of spherical micelles for the sample prepared and dried at 60 °C. The micelle cores are slightly anisotropic and show a higher phase contrast compared to that of the corona, which is attributed to the crystallinity of the PE core and the presence of a large amount of free chains forming a continuous layer on the silicon wafer (Figure 5B). SFM measurements were conducted at room temperature after the sample was completely dried at 60 °C; i.e., PE is able to crystallize in the core of the dried micelles. Thus, the crystalline core is a matter of sample preparation and not attributed to the existence of micelles with a crystalline core at 60 °C in solution. The SFM results are in agreement with DLS investigations, showing the coexistence of unimers and micelles at 80 and 60 °C (Figure S2 in the Supporting Information). After cooling the solution to 20 °C (parts C and D of Figure 5), wormlike aggregates were formed, having a comparable length and diameter with respect to wormlike micelles obtained at higher concentrations (Figure 3). This supports the proposed mechanism, i.e., crystallization-induced aggregation of spherical micelles to wormlike structures upon cooling.

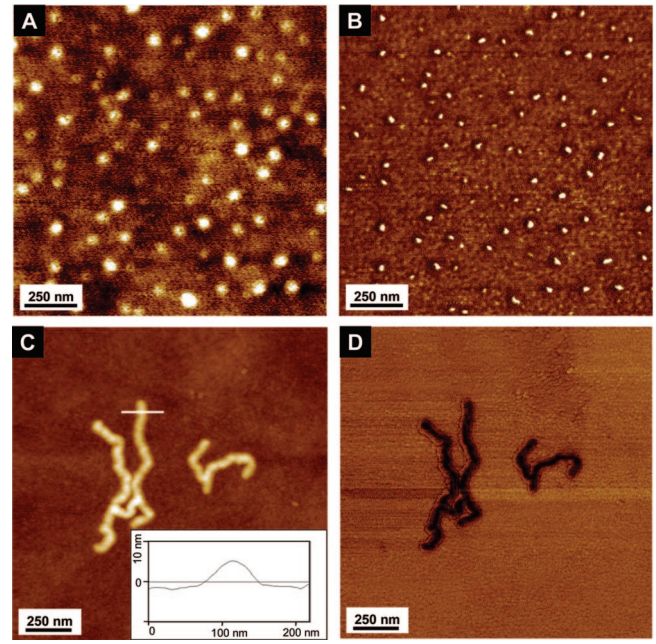

Figure 5. SFM topography and phase-contrast images of $S_{39}E_{21}M_{40}^{91.5}$ aggregates deposited onto a silicon wafer by dip coating from a 0.05 g/L toluene solution at 60 °C (A, z range = 5 nm; B, $\Delta\varphi = 10°$), and after subsequent cooling at 20 °C (C, z range = 20 nm; D, $\Delta\varphi = 30°$). The inset in C shows a section analysis of the formed wormlike micelle (white bar indicates the analyzed region).

A strong effect of molecular weight on the formed structure was reported for poly(ethylene oxide)-*block*-poly(butylene oxide) (PEO-*b*-PBO, 55 wt % PEO) diblock copolymers in solution and blends with low-molecular-weight PBO.[36] High-molecular-weight PEO-*b*-PBO diblock copolymers formed spherical micelles, whereas samples with identical composition but lower M_n formed platelet-like structures. This was explained by an "over-spilling" effect[6] of the coronal chains, shielding the lateral surfaces of the formed crystallites and thus preventing further aggregation. Consequently, one would expect that the high molecular weight of the $S_{39}E_{21}M_{40}^{91.5}$ triblock terpolymer in combination with the low content of crystallizable PE (21 wt %) favors the formation of spherical rather than wormlike micelles. Here, the incompatibility of the coronal PS and PMMA chains, resulting in a less effective shielding, might be a possible explanation for the observed aggregation into wormlike micelles. Additionally, the intrinsic chain folding within the PE crystallites

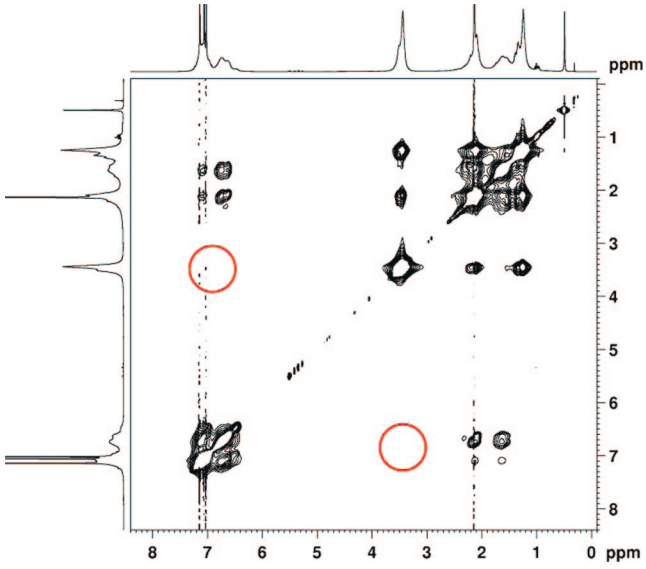

Figure 6. Contour plot of a 2D ^{1}H NOESY experiment on $S_{39}E_{21}M_{40}^{91.5}$ in toluene-d_8 (10 g/L). The circles indicate the positions where cross-peaks because of close proximity of PS and PMMA segments should be expected.

(caused by ethyl branches) decreases the grafting density of coronal chains on the fold surface; i.e., the free-energy penalty for chain stretching in the case of densely grafted chains is reduced, favoring a lower curvature.[5]

Structure of the Corona. To check the microphase separation within the corona of the wormlike micelles in solution, we have performed 2D ^{1}H NOESY. This method has been recently implemented to prove the Janus-type structure of micelles; i.e., the micelle corona consists of two microphase-separated faces.[38] ^{1}H NMR NOESY is a two-dimensional NMR technique probing internuclear distances. When two protons of chemically different monomers are in close proximity (distances < 0.5 nm) cross-peaks will be present in the 2D ^{1}H NMR spectrum, because of magnetization transfer by cross-relaxation, which scales with r^{-6} (where r is the internuclear distance between the protons).

Figure 6 shows the contour plot of a 2D ^{1}H NOESY experiment on $S_{39}E_{21}M_{40}^{91.5}$ wormlike micelles recorded with an ultrahigh sensitive 800 MHz NMR spectrometer equipped with a cryogenically cooled probe. Clearly, no cross-peaks (circles indicate position where cross-peaks should occur in the case of close proximity) were observed between ^{1}H NMR signals of PS [$\delta = 6.5$–7.5 ppm (aromatic protons)] and PMMA [$\delta = 3.5$ ppm ($-O-CH_3$)], pointing to a microphase separation between PS and PMMA chains in the corona. This is supported by a recent report on semiconductor quantum dots stabilized via adsorption of a PS-*b*-PAA-*b*-PMMA [PAA = poly(acrylic acid)] triblock terpolymer. Two-dimensional ^{1}H NOESY experiments showed cross-peaks between PS and PMMA, indicating a mixed PS/PMMA corona.[39] This clearly shows the applicability of this method; i.e., cross-peaks can be observed in the case of a mixed PS/PMMA corona. However, 2D ^{1}H NOESY is not able to distinguish between a Janus-type (two-faced) or patched[26] (multiple PS and PMMA compartments) configuration in the corona.

We have studied the aggregation of the wormlike micelles in acetone, a good solvent for PMMA and a nonsolvent for PS, to obtain a closer insight into the structure of the corona. The acetone solution was obtained by dialysis of a 1 g/L toluene solution of the triblock terpolymer against acetone (see the Experimental Section). A strong aggregation of the wormlike micelles, if they are Janus-type, might be expected because of the insolubility of the PS blocks. For Janus cylinders, prepared via cross-linking in the bulk state of a SBM triblock terpolymer with a lc morphology, a significantly increased height in SFM images was observed and attributed to strong aggregation in acetone.[28] On the other hand, for a mixed shell of PS and PMMA, the micelles should be well-dispersed. Figure 7A shows a TEM micrograph of the aggregates formed in acetone. Obviously, only segments of the wormlike micelles are aggregated, resulting in the formation of loosely bound assemblies. Furthermore, aggregation does not span over the entire length, as might be expected for a Janus-type configuration. This strongly supports a patched structure of the corona.

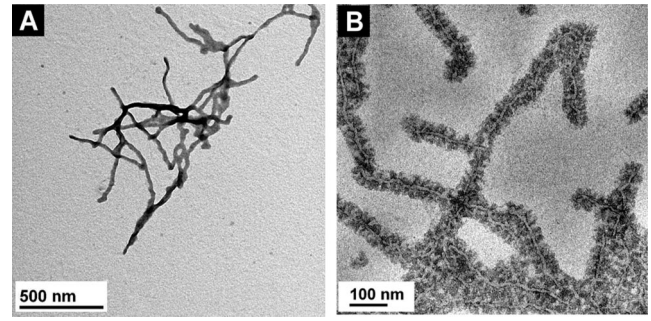

Figure 7. TEM micrographs of $S_{39}E_{21}M_{40}^{91.5}$ wormlike micelles: (A) aggregates formed in acetone (0.5 g/L), a selective solvent for PMMA, and (B) drop coated from toluene solution (0.5 g/L) followed by selective staining of the PS domains with RuO_4 for 60 min.

Selective staining of the PS domains with RuO_4 was used to verify the concept of a patched corona (Figure 7B). The sample was first drop coated onto a carbon-coated copper grid (0.5 g/L in toluene), followed by staining with RuO_4 vapor for 60 min. Well-separated dark areas (higher scattering contrast), corresponding to stained PS domains, can be detected along the long axis of the wormlike micelles. This result clearly proves the patch-like structure of the corona. The crystalline PE domains in the core appear bright because of the preferential staining of the amorphous fold interface between core and corona.

Structure of the Core. Because of the chain packing in the crystalline PE cores, the structure of the core might be expected to reflect the shape of a rectangular prism rather than that of a cylinder, even though the overall structure of the micelle is wormlike (cylindrical).[5] This is supported by the TEM micrograph in Figure 2B. In some areas, dark domains, i.e., higher scattering contrast with respect to that of the corona, corresponding to the crystalline core, are clearly visible, whereas in other areas, the contrast almost vanishes. In the case of a cylindrical core, the contrast is expected to be constant over the complete length. Because of the small size of the crystalline PE core, it was not possible to conduct electron diffraction, which would give more detailed information about the chain packing in the core. However, WAXD on a $S_{39}E_{21}M_{40}^{91.5}$ solution in toluene (50 g/L) revealed a principal peak at $q \approx 14.8$ nm^{-1}, which can be assigned to the Bragg peak of the [110] plane in the usually observed orthorhombic crystal structure of PE (Figure 8).[40] Thus, chain packing within the semicrystalline PE core is comparable to that in bulk PE. The second characteristic Bragg peak ([200]) cannot be detected unambiguously, most likely because of the low scattering intensity. This might be attributed to the low content of PE in the solution (ca. 1 wt %) combined with the rather low degree of crystallinity [for bulk sample, α(PE) = 24.9%].

For rodlike micelles with a crystalline PFDMS core, the core was proposed to consist of a monolayer ribbon of PFDMS chains.[20] However, this model is not applicable in our case, because this cannot explain the significantly higher contrast observed in TEM for the PE core with respect to the corona. It is more likely that the structure of the core resembles a

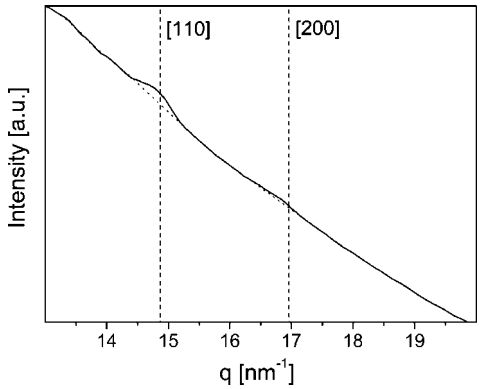

Figure 8. WAXD pattern obtained for a toluene solution of $S_{39}E_{21}M_{40}^{91.5}$ (50 g/L) after cooling from 60 to 20 °C. The dashed lines indicate the expected Bragg peaks ([110] and [200]) for PE in its orthorhombic modification.

rectangular prism twisted along the long axis, which would account for the observed contrast variations. A similar structure, denoted as nanostructured bands, was reported for poly(L-lactide)-*block*-poly(ethylene oxide) block copolymers on mica surfaces after annealing.[23] Extensive scattering experiments are necessary to elucidate the exact structure of the crystalline core, which will be the focus of upcoming investigations.

Conclusions

We have observed an unexpected formation of wormlike micelles for a PS-*b*-PE-*b*-PMMA triblock terpolymer ($S_{39}E_{21}M_{40}^{91.5}$) via crystallization-induced aggregation upon cooling in organic media. TEM showed that the wormlike micelles have a core−corona structure, consisting of a semicrystalline PE core and a corona built up by the soluble PS and PMMA chains. Two-dimensional ^{1}H NOESY combined with TEM investigations on selectively stained samples revealed a patched structure of the corona. Initial studies on the aggregation mechanism using temperature-dependent DLS and SFM in combination with DSC pointed to a crystallization-induced aggregation of spherical micelles upon cooling. Further studies are ongoing to obtain a deeper insight into the aggregation mechanism, the structure of the core, and the influence of molecular weight and composition of the triblock terpolymer on the structure formed.

Our initial results show that crystallization-induced self-assembly of ABC triblock terpolymers in solution might open an alternative route to polymer nanostructures with a microphase-separated corona. When the composition and/or molecular weight of the triblock terpolymer is adjusted, control over the type of structure formed, i.e., spherical, wormlike (cylindrical), or lamellar, should be feasible. Moreover, varying the chemistry of the A and C blocks not only the microphase separation in the corona but also the amphiphilicity can be easily tuned, making these systems very interesting for hierarchical self-assembly studies.

Acknowledgment. We thank Dieter Gräbner (University of Bayreuth, BZKG) for conducting the micro-DSC measurements and Markus Ruppel (Imperial College London, Department of Chemical Engineering) for assistance with the light scattering experiments. Support of Arnaud Chiche (University of Bayreuth, PC I) and Emanuela Di Cola (ESRF, Grenoble) concerning the WAXD measurements is gratefully acknowledged. This work was partially supported by the German Science Foundation (Collaborative Research Center 481) and the European Union (EU) within the Marie Curie RTN POLYAMPHI.

Supporting Information Available: Additional temperature- and time-dependent dynamic light scattering results. This material is available free of charge via the Internet at http://pubs.acs.org.

References and Notes

(1) (a) Gohy, J.-F. *Adv. Polym. Sci.* **2005**, *190*, 65–136. (b) Hadjichristidis, N.; Iatrou, H.; Pitsikalis, M.; Pispas, S.; Avgeropoulos, A. *Prog. Polym. Sci.* **2005**, *30*, 725–782. (c) Rodríguez-Hernández, J.; Chécot, F.; Gnanou, Y.; Lecommandoux, S. *Prog. Polym. Sci.* **2005**, *30*, 691–724 .

(2) (a) Antonietti, M.; Förster, S. *Adv. Mater.* **2003**, *15*, 1323–1333. (b) Discher, D. E.; Eisenberg, A. *Science* **2002**, *297*, 967–972. (c) Soo, P. L.; Eisenberg, A. *J. Polym. Sci., Part B: Polym. Phys.* **2004**, *42*, 923–938. (d) Bhargava, P.; Tu, Y.; Zheng, J. X.; Xiong, H.; Quirk, R. P.; Cheng, S. Z. D. *J. Am. Chem. Soc.* **2007**, *129*, 1113–1121. (e) Bhargava, P.; Zheng, J. X.; Li, P.; Quirk, R. P.; Harris, F. W.; Cheng, S. Z. D. *Macromolecules* **2006**, *39*, 4880–4888. (f) Chen, E.-Q.; Xia, Y.; Graham, M. J.; Foster, M. D.; Mi, Y.; Wu, W.-L.; Cheng, S. Z. D. *Chem. Mater.* **2003**, *15*, 2129–2135. (g) Choucair, A.; Eisenberg, A. *Eur. Phys. J. E* **2003**, *10*, 37–44. (h) Zhang, L.; Eisenberg, A. *Polym. Adv. Technol.* **1998**, *9*, 677–699. (i) Zhang, L.; Yu, K.; Eisenberg, A. *Science* **1996**, *272*, 1777–1779. (j) Zhang, L.; Eisenberg, A. *Science* **1995**, *268*, 1728–1731.

(3) (a) Yan, X.; Liu, G.; Li, H. *Langmuir* **2004**, *20*, 4677–4683. (b) Borsali, R.; Minatti, E.; Putaux, J.-L.; Schappacher, M.; Deffieux, A.; Viville, P.; Lazzaroni, R.; Narayanan, T. *Langmuir* **2003**, *19*, 6–9. (c) Jain, S.; Bates, F. S. *Science* **2003**, *300*, 460–464. (d) Won, Y.-Y.; Davis, H. T.; Bates, F. S. *Science* **1999**, *283*, 960–963.

(4) (a) Cui, H.; Chen, Z.; Wooley, K. L.; Pochnan, D. J. *Macromolecules* **2006**, *39*, 6599–6607. (b) Lei, L.; Gohy, J.-F.; Willet, N.; Zhang, J.-X.; Varshney, S.; Jérôme, R. *Macromolecules* **2004**, *37*, 1089–1094. (c) Yan, X.; Liu, G.; Li, Z. *J. Am. Chem. Soc.* **2004**, *126*, 10059–10066. (d) Liu, F.; Liu, G. *Macromolecules* **2001**, *34*, 1302–1307. (e) Stewart, S.; Liu, G. *Angew. Chem., Int. Ed.* **2000**, *39*, 340–344. (f) Yu, G.-E.; Eisenberg, A. *Macromolecules* **1998**, *31*, 5546–5549.

(5) Vilgis, T.; Halperin, A. *Macromolecules* **1991**, *24*, 2090–2095.

(6) Halperin, A. Polymeric vs. Monomeric Amphiphiles: Design Parameters. In *Supramolecular Polymers*; Ciferri, A., Ed.; Marcel Dekker: New York, 2000; pp 93–146.

(7) Williams, D. R. M.; Fredrickson, G. H. *Macromolecules* **1992**, *25*, 3561–3568.

(8) Lin, E. K.; Gast, A. P. *Macromolecules* **1996**, *29*, 4432–4441.

(9) (a) Monkenbusch, M.; Schneiders, D.; Richter, D.; Willner, L.; Leube, W.; Fetters, L. J.; Huang, J. S.; Lin, M. *Physica B* **2000**, *276–278*, 941–943. (b) Ramzi, A.; Prager, M.; Richter, D.; Efstratiadis, V.; Hadjichristidis, N.; Young, R. N.; Allgaier, J. B. *Macromolecules* **1997**, *30*, 7171–7182. (c) Richter, D.; Schneiders, D.; Monkenbusch, M.; Willner, L.; Fetters, L. J.; Huang, J. S.; Lin, M.; Mortensen, K.; Farago, B. *Macromolecules* **1997**, *30*, 1053–1068.

(10) Schwahn, D.; Richter, D.; Wright, P. J.; Symon, C.; Fetters, L. J.; Lin, M. *Macromolecules* **2002**, *35*, 861–870.

(11) (a) Chen, W. Y.; Li, C. Y.; Zheng, J. X.; Huang, P.; Zhu, L.; Ge, Q.; Quirk, R. P.; Lotz, B.; Deng, L.; Wu, C.; Thomas, E. L.; Cheng, S. Z. D. *Macromolecules* **2004**, *37*, 5292–5299. (b) Gast, A. P.; Vinson, P. K.; Cogan-Farinas, K. A. *Macromolecules* **1993**, *26*, 1774–1776. (c) Zheng, J. X.; Xiong, H.; Chen, W. Y.; Lee, K.; Van Horn, R. M.; Quirk, R. P.; Lotz, B.; Thomas, E. L.; Shi, A.-C.; Cheng, S. Z. D. *Macromolecules* **2006**, *39*, 641–650.

(12) Cogan, K. A.; Gast, A. P. *Macromolecules* **1990**, *23*, 745–753.

(13) (a) Lee, M.; Cho, B.-K.; Zin, W.-C. *Chem. Rev.* **2001**, *101*, 3869–3892. (b) Liang, Y.; Wang, H.; Yuan, S.; Lee, Y.; Gan, L.; Yu, L. *J. Mater. Chem.* **2007**, *17*, 2183–2194.

(14) Portinha, D.; Boué, F.; Bouteiller, L.; Carrot, G.; Chassenieux, C.; Pensec, S.; Reiter, G. *Macromolecules* **2007**, *40*, 4037–4042.

(15) Slager, J.; Brizzolara, D.; Cantow, H. J.; Domb, A. J. *Polym. Adv. Technol.* **2005**, *16*, 667–674.

(16) (a) Cao, L.; Manners, I.; Winnik, M. A. *Macromolecules* **2002**, *35*, 8258–8260. (b) Gohy, J.-F.; Lohmeijer, B. G. G.; Alexeev, A.; Wang, X.-S.; Manners, I.; Winnik, M. A.; Schubert, U. S. *Chem.—Eur. J.* **2004**, *10*, 4315–4323. (c) Wang, X.; Winnik, M. A.; Manners, I. *Macromolecules* **2005**, *38*, 1928–1935.

(17) Korczagin, I.; Hempenius, M. A.; Fokkink, R. G.; Cohen Stuart, M. A.; Al-Hussein, M.; Bomans, P. H. H.; Frederik, P. M.; Vancso, G. J. *Macromolecules* **2006**, *39*, 2306–2315.

(18) Massey, J. A.; Temple, K.; Cao, L.; Rharbi, Y.; Raez, J.; Winnik, M. A.; Manners, I. *J. Am. Chem. Soc.* **2000**, *122*, 11577–11584.

(19) Wang, H.; Winnik, M. A.; Manners, I. *Macromolecules* **2007**, *40*, 3784–3789.

(20) Guérin, G.; Raez, J.; Manners, I.; Winnik, M. A. *Macromolecules* **2005**, *38*, 7819–7827.

(21) (a) Raez, J.; Barjovanu, R.; Massey, J. A.; Winnik, M. A.; Manners, I. *Angew. Chem., Int. Ed.* **2000**, *39*, 3862–3865. (b) Raez, J.; Tomba,

J. P.; Manners, I.; Winnik, M. A. *J. Am. Chem. Soc.* **2003**, *125*, 9546–9547.
(22) (a) Dröscher, M.; Smith, T. L. *Macromolecules* **1982**, *15*, 442–449. (b) Kawai, T.; Shiozaki, S.; Sonoda, S.; Nakagawa, H.; Matsumoto, T.; Maeda, H. *Angew. Makromol. Chem.* **1969**, *128*, 252–262.
(23) (a) Fujiwara, T.; Kimura, Y. *Macromol. Biosci.* **2002**, *2*, 11–23. (b) Fujiwara, T.; Miyamoto, M.; Kimura, Y.; Iwata, T.; Doi, Y. *Macromolecules* **2001**, *34*, 4043–4050.
(24) (a) Resendes, R.; Massey, J. A.; Dorn, H.; Power, K. N.; Winnik, M. A.; Manners, I. *Angew. Chem., Int. Ed.* **1999**, *38*, 2570–2573. (b) Resendes, R.; Massey, J. A.; Temple, K.; Cao, L.; Power-Billard, K. N.; Winnik, M. A.; Manners, I. *Chem.—Eur. J.* **2001**, *7*, 2414–2424.
(25) Wang, X. S.; Winnik, M. A.; Manners, I. *Macromolecules* **2002**, *35*, 9146–9150.
(26) (a) Hoppenbrouwers, E.; Li, Z.; Liu, G. *Macromolecules* **2003**, *36*, 876–881. (b) Kuo, S.-W.; Tung, P.-H.; Lai, C.-L.; Jeong, K.-U.; Chang, F.-C. *Macromol. Rapid Commun.* **2008**, *29*, 229–233.
(27) (a) Erhardt, R.; Böker, A.; Zettl, H.; Kaya, H.; Pyckhout-Hintzen, W.; Krausch, G.; Abetz, V.; Müller, A. H. E. *Macromolecules* **2001**, *34*, 1069–1075. (b) Erhardt, R.; Zhang, M.; Böker, A.; Zettl, H.; Abetz, C.; Frederik, P.; Krausch, G.; Abetz, V.; Müller, A. H. E. *J. Am. Chem. Soc.* **2003**, *125*, 3260–3267. (c) Walther, A.; André, X.; Drechsler, M.; Abetz, V.; Müller, A. H. E. *J. Am. Chem. Soc.* **2007**, *129*, 6187–6198.
(28) Liu, Y.; Abetz, V.; Müller, A. H. E. *Macromolecules* **2003**, *36*, 7894–7898.
(29) (a) Ishizu, K.; Toyoda, K.; Furukawa, T.; Sogabe, A. *Macromolecules* **2004**, *37*, 3954–3957. (b) Ishizu, K.; Yamada, H. *Macromolecules* **2007**, *40*, 3056–3061. (c) Stephan, T.; Muth, S.; Schmidt, M. *Macromolecules* **2002**, *35*, 9857–9860.
(30) Ruckdäschel, H.; Sandler, J. K. W.; Altstädt, V.; Rettig, C.; Schmalz, H.; Abetz, V.; Müller, A. H. E. *Polymer* **2006**, *47*, 2772–2790.
(31) Brandrup, J.; Immergut, E. H., *Polymer Handbook*, 3rd ed.; Wiley: New York, 1989.
(32) (a) Schmalz, H.; Böker, A.; Lange, R.; Krausch, G.; Abetz, V. *Macromolecules* **2001**, *34*, 8720–8729. (b) Schmalz, H.; Knoll, A.; Müller, A. J.; Abetz, V. *Macromolecules* **2002**, *35*, 10004–10013.
(33) Berdyyeva, T.; Woodworth, S. D.; Sokolov, I. *Ultramicroscopy* **2005**, *102*, 189–198.
(34) Satija, K. S.; Majkrzak, C. F.; Russell, T. P.; Sinha, S. K.; Sirota, E. B.; Hughes, G. J. *Macromolecules* **1990**, *23*, 3860–3864.
(35) (a) Beers, K. L.; Gaynor, S. G.; Matyjaszewski, K.; Sheiko, S. S.; Möller, M. *Macromolecules* **1998**, *31*, 9413–9415. (b) Cheng, G.; Böker, A.; Zhang, M.; Krausch, G.; Müller, A. H. E. *Macromolecules* **2001**, *34*, 6883–6888. (c) Dziezok, P.; Sheiko, S. S.; Fischer, K.; Schmidt, M.; Möller, M. *Angew. Chem., Int. Ed.* **1997**, *36*, 2812–2815. (d) Xu, Y.; Becker, H.; Yuan, J.; Burkhardt, M.; Zhang, Y.; Walther, A.; Bolisetty, S.; Ballauff, M.; Müller, A. H. E. *Macromol. Chem. Phys.* **2007**, *208*, 1666–1675.
(36) (a) Xu, J.-T.; Fairclough, J. P. A.; Mai, S.-M.; Ryan, A. J. *J. Mater. Chem.* **2003**, *13*, 2740–2748. (b) Xu, J.-T.; Jin, W.; Liang, G.-D.; Fan, Z.-Q. *Polymer* **2005**, *46*, 1709–1716.
(37) Raez, J.; Manners, I.; Winnik, M. A. *J. Am. Chem. Soc.* **2002**, *124*, 10381–10395.
(38) Voets, I. K.; de Keizer, A.; de Waard, P.; Frederik, P. M.; Bomans, P. H. H.; Schmalz, H.; Walther, A.; King, S. M.; Leermakers, F. A. M.; Cohen Stuart, M. A. *Angew. Chem., Int. Ed.* **2006**, *45*, 6673–6676.
(39) Guo, Y.; Moffitt, M. G. *Macromolecules* **2007**, *40*, 5868–5878.
(40) (a) Bunn, C. W. *Trans. Faraday Soc.* **1939**, *35*, 482–491. (b) Weimann, P. A.; Hajduk, D. A.; Chu, C.; Chaffin, K. A.; Brodil, J. C.; Bates, F. S. *J. Polym. Sci., Part B: Polym. Phys.* **1999**, *37*, 2053–2068.

MA702417Y